Abnormal charge injection behavior at metal-organic interfaces

Z. B. Wang,* M. G. Helander, S. W. Tsang, and Z. H. Lu†
Department of Materials Science and Engineering, University of Toronto, 184 College Street, Toronto, Ontario, Canada M5S 3E4
(Received 7 September 2008; published 6 November 2008)

Charge injection physics at metal-organic interfaces with barrier heights of 0.6–1.5 eV has been systematically studied. It is discovered that for sufficiently high barriers the injection current becomes temperature independent. The phenomenon contradicts the orthodox charge injection theory that predicts a simple exponential temperature dependence of charge injection. To explain the observed experimental results, tunneling injection via interfacial traps is proposed. The relative impact of various parameters such as trap density, energy level, and energy disorder is studied. The theoretical calculations indicate that interfacial deep traps, even of trivial amount, will have a huge impact on charge injection at various temperatures. Therefore trap states at the interface should be considered whenever barrier height is to be extracted from *I-V* curves at various temperatures.

DOI: 10.1103/PhysRevB.78.193303 PACS number(s): 73.20.−r, 71.10.−w, 73.40.Sx, 73.61.Ph

Organic electronics is a rapidly expanding research field and has numerous applications such as organic light-emitting diodes (OLEDs),[1–4] organic thin-film transistors,[5,6] organic photovoltaics (OPV),[7,8] and organic memory devices.[9,10] However, despite its rapid industrial application over the last few decades, fundamental charge injection physics for organic semiconductors is still poorly understood. Since organic semiconductors contain almost no intrinsic charge carriers, devices operate solely on charges injected from the electrodes.[11] Hence, understanding of the physics that governs injection at metal-organic interfaces (MOIs) is crucial to organic electronics. Based on the hopping model proposed by Bässler,[12] several studies have been conducted to either improve the injection model[13] or to extract useful parameters based on the injection model.[14–16] In the latter case, injection barrier heights for holes or electrons are extracted by modeling electrical characteristics at various temperatures. However, if the temperature dependence deviates from the exponential dependence $\exp(-\phi/kT)$, where ϕ is the effective barrier height, k is the Boltzmann constant, and T is the temperature, the value of injection barrier derived from the model will be dubious. In this Brief Report, we report on an abnormal temperature-independent charge injection at MOIs that deviates significantly from the temperature dependence predicted by any model. Tunneling injection via interfacial deep trap states is proposed to explain the observed phenomena. In traditional inorganic semiconductors, a similar concept of trap-assisted injection has been proposed;[17,18] however, it is well known that organic semiconductors are different from the inorganic semiconductors since the states are highly localized in organics. In this work, we present the impact of traps at metal/organic interfaces.

The single-carrier hole-only devices in this work were fabricated on Corning® 1737 glass substrates (50 $\times$ 50 mm^2) using a Kurt J. Lesker LUMINOS® cluster tool with a base pressure of $\sim 10^{-8}$ Torr. Organic and metal films were deposited in separate chambers without breaking vacuum. The anode metals used in this study were Au, Co, Cu, Ag, Al, and Mg. Au was used as the cathode contact metal to minimize electron injection due to its high work function. To eliminate the possible diffusion of cathode metal into the organic layer during deposition, the Au evaporation boat was heat shielded and the source to substrate distance was ~65 cm. Since the thickness of each organic layer is crucial in the study of single-carrier devices, film thicknesses were monitored by a calibrated quartz-crystal microbalance (QCM) and were further verified for each sample by using both a stylus profilometer (KLA Tencor P-16+) and capacitance-voltage (*C-V*) measurements (Agilent 4294A). Current-voltage (*I-V*) characteristics were measured in a closed-loop low-temperature cryostat with a base pressure of $\sim 10^{-6}$ Torr using an HP4140B picoammeter. In order to ensure that the current density measured at low temperature is not due to leakage current, we also measured the leakage current of the system. The leakage current density with a correction of the active area of the devices (2 mm^2) was found to be $\sim 10^{-12}$ A cm^{-2}, which is several orders of magnitude lower than the measured current density of the devices.

Figure 1 shows current density as a function of electric field at different temperatures in the range 100–300 K for hole-only single-carrier devices where the organic film is made of 4,4′,4″-tris(N-3-methylphenyl-N-phenyl-amino) triphenylamine (*m*-MTDATA) and the anodes are made of Au, Mg, and Mg/C_{60}, respectively. The current density for devices with the Mg anode [Fig. 1(b)] exhibits almost no temperature dependence. This is in stark contrast to the exponential temperature dependence predicted by typical charge injection models[13,19] involving thermal processes. Clearly none of the thermionic emission-based models can account for the temperature *independence* observed for Mg anode devices. It is well known that the injection current described by Fowler-Nordheim (FN) tunneling[20] is independent of temperature, i.e., it has no term related to temperature. However, FN is only applicable at extremely high fields;[19] the electric fields discussed in this Brief Report are substantially lower, as is the case for most organic electronic devices ($\sim 5 \times 10^5$ V/cm) such as OLEDs. What is more, FN theory is also very simplistic as little consideration has been given to the fact that the final states are localized,[19] which is an inherent nature of organic semiconductors. Arkhipov *et al.*[13] proposed a two-step hopping model that considers the energy disorder of the localized states. However, this model predicts much stronger temperature dependence than the data we observed here [Fig. 1(b)].

In addition to the abnormal temperature dependence of

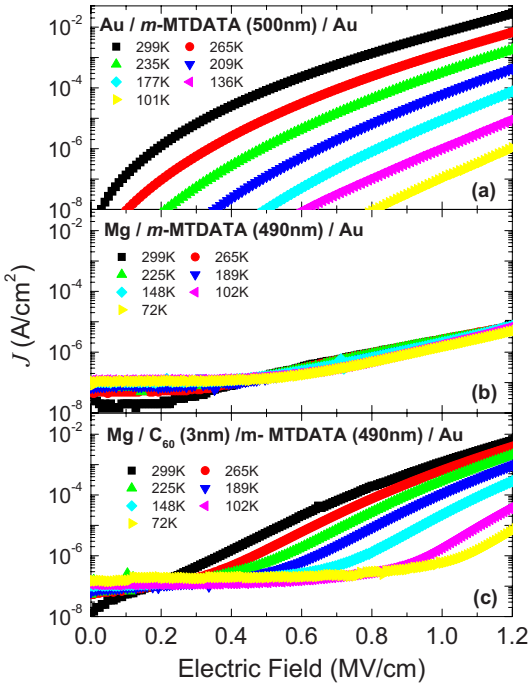

FIG. 1. (Color online) Current density as a function of electric field at various temperatures measured on hole-only single-carrier devices made from *m*-MTDATA with (a) Au, (b) Mg, and (c) Mg/C_{60} anodes.

the injection current for Mg devices, we also observed an abnormal trend in temperature dependence as a function of injection barrier. In other words, the temperature dependence for higher barriers is observed to deviate from the trend predicted by any of the previously discussed models (i.e., increasing temperature dependence with barrier height). Figure 1 shows the temperature dependence of the injection current for devices with three different barriers, namely, the Mg, Mg/C_{60}, and Au anodes. It is believed that an interfacial dipole exists at MOIs,[21] which may change the effective barrier for injection. The work function of Mg is approximately 1.3 eV lower than that of Au. Accounting for dipole effects, the injection barrier for Mg/*m*-MTDATA is still much larger than for Au/*m*-MTDATA. However, as indicated in Fig. 1, the Au anode devices are significantly more temperature dependent than Mg. Figure 1(c) shows another case using a Mg/C_{60} anode. The work function of which is increased over Mg due to the surface modification by C_{60}.[22,23] The order of injection barriers is as follows: $Mg > Mg/C_{60} > Au$. This ordering is in good agreement with the room-temperature current densities for the three different anodes. However, in terms of temperature dependence, this ordering is reversed and contradictive to the models mentioned above, i.e., the temperature dependence decreases instead of increases for higher barrier. Results for other anodes (Co, Cu, Ag, and Al) are summarized in Fig. 2.

Figure 2 plots the relative temperature dependence as a function of injection barrier. Here the relative temperature dependence is defined as the ratio of room-temperature current density $J_{300\ K}$ to the current density at 200 K, $J_{200\ K}$, at a constant electric field of 5×10^5 V/cm. This normalized value $J_{300\ K}/J_{200\ K}$ reflects the temperature dependence over

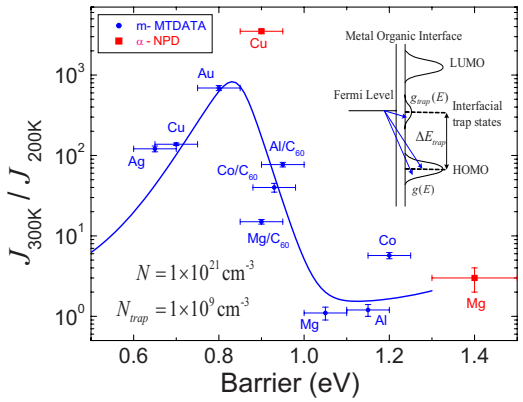

FIG. 2. (Color online) Relative current ratio $J_{300\ K}/J_{200\ K}$ as a function of injection barrier at a constant electric field of 5×10^{-5} V/cm. The solid line is the calculated curve with the consideration of tunneling to interface trap states. The inset is a schematic of the proposed injection process with the consideration of trap states at the interface.

a range of 100 K. The injection barriers for various MOIs are estimated from the room-temperature current densities (shown in Fig. 3), which accounts for both the offset between highest occupied molecular orbital (HOMO) in the organic and the Fermi level in metal and any dipole effects at the interface. The reason for choosing 200 K as the reference current density is that the various bulk transport parameters of organic thin films may change at extremely low temperature below 200 K. For example, in the case of *m*-MTDATA, when the temperature is below 100 K, the measured mobility deviates from the Gaussian disorder model (GDM). Figure 2 shows that the relative temperature dependence increases with increasing barrier height from ~0.6 to ~0.8 eV. The relative temperature dependence, however, starts to decrease with increasing barrier from ~0.8 to ~1 eV, and for barrier heights >1 eV the current density becomes completely independent of temperature. In Fig. 3 the space-charge limited current[24] is also calculated using measured mobility values of *m*-MTDATA from Ref. 25, which is found to be orders of

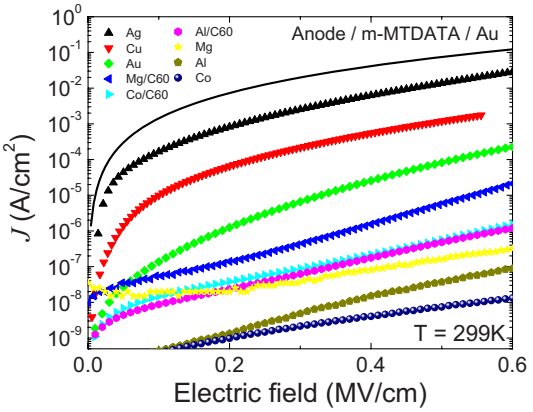

FIG. 3. (Color online) Current density as a function of electric field at room temperature for *m*-MTDATA devices with various anodes as labeled. The solid curve is the calculated space-charge limited current of a 500-nm-thick *m*-MTDATA device using measured mobility values.

magnitude higher than the current density with different anodes. This indicates that with a thick organic layer (500 nm) the current is still injection limited for all devices.

The proposed injection process with a consideration of trap state tunneling is shown in the inset of Fig. 2. In this process the injection current is a sum of hopping rates from the Fermi level of the metal to both the HOMO and trap states in the organic. The proposed mechanism is derived based on the hopping model.[13] In the original model the injection limited current is described by the following formulation:[13]

$$J_{\mathrm{inj}} \propto \int_{a}^{\infty} dx_0 w_{\mathrm{esc}}(x_0)\exp(-2\gamma x_0)\int_{-\infty}^{\infty} d\varepsilon\ \mathrm{Bol}(\varepsilon)g(\varepsilon - U), \quad (1)$$

where a is the nearest-neighbor distance, γ is the inverse localization radius, x_0 is the hopping distance, w_{esc} is the escape probability, $\mathrm{Bol}(E)$ is the energy dependence of the jump rate, and U is the energy difference between the Fermi level of the metal and the HOMO of the organic. The energy disorder in organic semiconductors is modeled as a Gaussian distribution of states as follows:

$$g(E) = (N/\sqrt{2\pi}\sigma)\exp[-(E^2/2\sigma^2)], \quad (2)$$

where N is the total spatial density of localized intrinsic molecular-orbital states and σ is the variance of the Gaussian distribution.

Trap states in organic semiconductors are often considered as deep localized states that exist between the HOMO and the lowest unoccupied molecular orbital (LUMO). The incorporation of both the intrinsic density of states and a distribution of traps was employed to study charge transport characteristics of the bulk.[26] Although the existence of traps in the bulk is generally accepted for practically all types of semiconductors, little consideration has previously been given to the effect of traps on the injection current. Including trap states the energy distribution in the organic is then

$$g'(E) = (N/\sqrt{2\pi}\sigma)\exp[-(E^2/2\sigma^2)] + g_{\mathrm{trap}}. \quad (3)$$

Here, a Gaussian distribution g_{trap} is also used to describe the trap states as

$$g_{\mathrm{trap}} = \frac{N_{\mathrm{trap}}}{\sqrt{2\pi}\sigma_{\mathrm{trap}}}\exp\left[-\frac{(E+\Delta E_{\mathrm{trap}})^2}{2\sigma_{\mathrm{trap}}^2}\right], \quad (4)$$

where ΔE_{trap} is the relative trap state energy level taken as the energy difference between the center of the HOMO and the center of the trap state distribution (see inset of Fig. 2); σ_{trap} is the variance of the Gaussian distribution of the trap states. Therefore the injection current is described by Eq. (1) with an energy distribution described by Eqs. (3) and (4).

In Fig. 2 the theoretical data shown in the solid line were calculated based on the model proposed above. The nearest-neighbor distance $a=0.5$ nm is taken as approximately half the size of the m-MTDATA molecule. The inverse localization radius is taken as $\gamma=3\times10^7$ cm^{-1}. The density of states in the HOMO ($N=10^{21}$ cm^{-3}) is taken by assuming one state per molecule. The energy disorder $\sigma=80$ meV is comparable to values measured by the time-of-flight (TOF) technique.[25] The temperature dependence is found to be very sensitive to the value of energy disorder. The other parameters related to the trap states used in the calculation are $\sigma_{\mathrm{trap}}=80$ meV, $N_{\mathrm{trap}}=10^9$ cm^{-3}, and $\Delta E_{\mathrm{trap}}=1.0$ eV. Figure 2 shows that the calculated curve (solid line) describes well the overall trend of relative temperature dependence as a function of barrier heights. This suggests the significance of deep trap states at the interface.

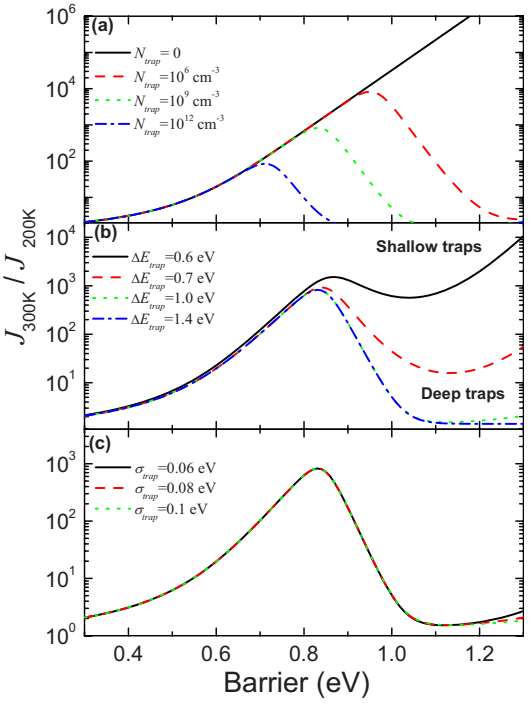

FIG. 4. (Color online) Calculated relative current ratio $J_{300\ \mathrm{K}}/J_{200\ \mathrm{K}}$ using various values of the trap state parameters: (a) density of trap states N_{trap}, (b) trap depth ΔE_{trap}, and (c) variance of trap states σ_{trap}.

On one hand, the injection current described by Eq. (1) is an integration of hopping rates from the metal into the first few monolayers of the organic. Since N_{trap} is much smaller (several orders of magnitude smaller) than N, the contribution to the current density from trap state tunneling is much less than the hopping rate to the HOMO especially at high temperature and small barrier. However, with increasing injection barrier the hopping rate exponentially decreases. Since the interfacial deep trap states are much deeper than the intrinsic localized states (i.e., ΔE_{trap} is large), the barrier to the trap states is much smaller than the barrier to the HOMO. Hence the carriers tend to fill the trap states prior to the HOMO. In other words, when the barrier to the HOMO is sufficiently high, the summation of the tunneling rates to the trap states may be equivalent to or even greater than that to the HOMO. As a result the contribution of the trap state tunneling becomes significant or even dominates in the total injection current as the barrier continues to increase. On the other hand, as mentioned previously the hopping model is thermionic assisted; hence, the lower the barrier height the less the injection current is expected to depend on temperature. Therefore the temperature dependence ($J_{300\ \mathrm{K}}/J_{\mathrm{T}}$) as a function of barrier will reach a maximum and then will de-

crease as a result of the two competing processes. After that $J_{300\ K}/J_T$ may increase again depending on the depth and density of the trap states, which will be discussed below.

With a fixed respective value of a, γ, N, and σ, the remaining uncertain parameters are σ_{trap}, N_{trap}, and ΔE_{trap}. Figure 4 shows the relative impact on $J_{300\ K}/J_{200\ K}$ of these parameters. Values of the other parameters are the same as discussed previously. From Fig. 4(a) it is clear that the onset of deviation from the thermionic model (in terms of barrier height) is highly dependent on N_{trap}. This indicates that the density of trap states plays a critical role in determining the injection current. For example, $N_{trap}=10^9$ cm^{-3} compared to $N=10^{21}$ cm^{-3} is many orders of magnitude lower and hence has been easily ignored in the past. However, such a small density of trap states can significantly change the injection current as has been shown previously in Fig. 2. Since even the purest organic materials have an intrinsic density of traps and impurities, it is necessary to consider the influence of the traps. Figure 4(b) also discusses the difference between deep traps and shallow traps. From the figure, we can see that the depth of the traps (in reference to HOMO) also has a significant influence on the injection current. The deviation of temperature dependence from the original hopping model increases as a function of trap depth. In contrast to the density of trap states and trap depth, the value of σ_{trap} does not significantly impact the current density [see Fig. 4(c)].

To demonstrate that the abnormal temperature dependence discussed above is universal (i.e., not limited to *m*-MTDATA), we also fabricated single-carrier hole-only devices with another commonly studied organic molecule N,N′-diphenyl-N, N′-bis-(1-naphthyl)-1-1′-biphenyl-4,4′-diamine (α-NPD). Two examples of Cu and Mg anodes are shown in Fig. 2 (red squares) in addition to the data for *m*-MTDATA. Clearly α-NPD devices follow a similar trend as *m*-MTDATA devices. Since the bulk parameters such as energy disorder for α-NPD are different from *m*-MTDATA, it is not proper to directly compare the α-NPD data to the solid curve calculated for *m*-MTDATA.

In conclusion, we demonstrate a significant deviation from the exponential temperature dependence predicted by traditional charge injection models based on thermally assisted injection processes. Tunneling injection via trap states is proposed. For sufficiently high injection barriers, the injection current was found to be independent of temperature. Calculations indicate that only a small density of deep traps is required to drastically alter the temperature dependence, which suggests the existence of interfacial trap states. Hence, the impact of trap states at the interface should be considered whenever barrier height is to be extracted from *I-V* curves at various temperatures.

We wish to acknowledge funding for this research by the Ontario Centres of Excellence and the Natural Sciences and Engineering Research Council (NSERC) of Canada.

*Corresponding author; zhibin.wang@utoronto.ca
†zhenghong.lu@utoronto.ca

[1] C. W. Tang and S. A. VanSlyke, Appl. Phys. Lett. **51**, 913 (1987).
[2] M. A. Baldo, D. F. O'Brien, Y. You, A. Shoustikov, S. Sibley, M. E. Thompson, and S. R. Forrest, Nature (London) **395**, 151 (1998).
[3] R. H. Friend, R. W. Gymer, A. B. Holmes, J. H. Burroughes, R. N. Marks, C. Taliani, D. D. C. Bradley, D. A. Dos Santos, J. L. Brédas, M. Lögdlund, and W. R. Salaneck, Nature (London) **397**, 121 (1999).
[4] J. Huang, M. Pfeiffer, A. Werner, J. Blochwitz, K. Leo, and S. Liu, Appl. Phys. Lett. **80**, 139 (2002).
[5] L. L. Chua, J. Zaumseil, J. F. Chang, E. C. W. Ou, P. K. H. Ho, H. Sirringhaus, and R. H. Friend, Nature (London) **434**, 194 (2005).
[6] L. Wang, M. H. Yoon, G. Lu, Y. Yang, A. Facchetti, and T. J. Marks, Nature Mater. **6**, 317 (2007).
[7] P. Peumans, S. Uchida, and S. R. Forrest, Nature (London) **425**, 158 (2003).
[8] G. Li, V. Shrotriya, J. Huang, Y. Yao, T. Moriarty, K. Emery, and Y. Yang, Nature Mater. **4**, 864 (2005).
[9] S. Möeller, C. Perlov, W. Jackson, C. Taussig, and S. R. Forrest, Nature (London) **426**, 166 (2003).
[10] J. Ouyang, C. W. Chu, C. R. Szmanda, L. Ma, and Y. Yang, Nature Mater. **3**, 918 (2004).
[11] H. Aziz, Z. D. Popovic, N. X. Hu, A. M. Hor, and G. Xu, Science **283**, 1900 (1999).
[12] H. Bässler, Phys. Status Solidi B **175**, 15 (1993).
[13] V. I. Arkhipov, E. V. Emelianova, Y. H. Tak, and H. Bässler, J. Appl. Phys. **84**, 848 (1998).
[14] J. K. J. van Duren, V. D. Mihailetchi, P. W. M. Blom, T. van Woudenbergh, J. C. Hummelen, M. T. Rispens, R. A. J. Janssen, and M. M. Wienk, J. Appl. Phys. **94**, 4477 (2003).
[15] J. Reynaert, V. I. Arkhipov, G. Borghs, and P. Heremans, Appl. Phys. Lett. **85**, 603 (2004).
[16] T. van Woudenbergh, P. W. M. Blom, M. Vissenberg, and J. N. Huiberts, Appl. Phys. Lett. **79**, 1697 (2001).
[17] C. Svensson and I. Lundström, J. Appl. Phys. **44**, 4657 (1973).
[18] M. Houssa, M. Tuominen, M. Naili, V. Afanas'ev, A. Stesmans, S. Haukka, and M. M. Heyns, J. Appl. Phys. **87**, 8615 (2000).
[19] J. C. Scott, J. Vac. Sci. Technol. A **21**, 521 (2003).
[20] R. H. Fowler and L. Nordheim, Proc. R. Soc. London **119**, 173 (1928).
[21] H. Ishii, K. Sugiyama, E. Ito, and K. Seki, Adv. Mater. (Weinheim, Ger.) **11**, 605 (1999).
[22] T. R. Ohno, Y. Chen, S. E. Harvey, G. H. Kroll, J. H. Weaver, R. E. Haufler, and R. E. Smalley, Phys. Rev. B **44**, 13747 (1991).
[23] N. Hayashi, H. Ishii, Y. Ouchi, and K. Seki, J. Appl. Phys. **92**, 3784 (2002).
[24] M. A. Lampert and P. Mark, *Current Injection in Solids* (Academic, New York, 1970).
[25] S. W. Tsang, M. W. Denhoff, Y. Tao, and Z. H. Lu, Phys. Rev. B **78**, 081301(R) (2008).
[26] E. V. Emelianova and G. J. Adriaenssens, J. Optoelectron. Adv. Mater. **6**, 1105 (2004).